Field-angle-dependent multi-frequency electron spin resonance spectroscopy in submillimeter wave range based on thermal detection

Takahashi, Hideyuki
Sakurai, Takahiro
Ohmichi, Eiji
Ohta, Hitoshi

(Citation)
Review of Scientific Instruments,92(8):083901

(Issue Date)
2021-08-01

(Resource Type)
journal article

(Version)
Version of Record

Review of Scientific Instruments ARTICLE scitation.org/journal/rsi

Field-angle-dependent multi-frequency electron spin resonance spectroscopy in submillimeter wave range based on thermal detection

Cite as: Rev. Sci. Instrum. 92, 083901 (2021); doi: 10.1063/5.0053227
Submitted: 6 April 2021 • Accepted: 15 July 2021 •
Published Online: 2 August 2021

Hideyuki Takahashi,[1,2,3,a)] Takahiro Sakurai,[4] Eiji Ohmichi,[3] and Hitoshi Ohta[1,3]

AFFILIATIONS

[1] Molecular Photoscience Research Center, Kobe University, 1-1 Rokkodai-cho, Nada, Kobe 657-8501, Japan
[2] JST-PRESTO, 4-1-8, Honcho, Kawaguchi-shi, Saitama 332-0012, Japan
[3] Graduate School of Science, Kobe University, 1-1 Rokkodai-cho, Nada, Kobe 657-8501, Japan
[4] Research Facility Center for Science and Technology, Kobe University, Kobe 657-8501, Japan

[a)] **Author to whom correspondence should be addressed:** hide.takahashi@crystal.kobe-u.ac.jp

ABSTRACT

We report the thermally detected electron spin resonance (ESR) spectroscopy in the frequency range of millimeter and submillimeter waves. Under high vacuum conditions, a cantilever-shaped device detects ESR absorption of a mounted sample as a temperature difference in its beam direction. Despite the simple experimental setup, the spin sensitivity of the order of 10^{12} spins/G was achieved at 10 K. The developed sample stage is small enough to be used in a 10 T split-pair superconducting magnet with a bore of 25 mm, enabling precise field-angle-dependent ESR measurements at multi-frequencies above 500 GHz. We demonstrate its usefulness by studying the field-angle dependence of the excitation energy of the dimer triplet state in the Shastry–Sutherland magnet $SrCu_2(BO_3)_2$.

I. INTRODUCTION

Electron spin resonance (ESR) provides microscopic insights into the environment around unpaired electrons through the g-tensor. In condensed matter, the g-tensor is generally anisotropic owing to the effects of local structure and interaction between spins. Furthermore, in magnetically ordered materials, the resonance frequency largely changes depending on the direction of the applied magnetic field.

Angle-dependent ESR can be performed by commercial ESR spectrometers based on the cavity perturbation method while using the sample rotation mechanism.[1] However, this method is not easy to perform in the frequency range above 100 GHz where the cavity volume is too small. The transmission type ESR is also not suitable for precise control of the magnetic field direction because it is difficult to combine the rigid waveguide circuit and a sample rotation mechanism in a narrow bore of a magnetic coil.[2] Despite these difficulties, angle rotation methods have been developed because of high demand. Most of these methods are based on the resonator techniques;[3–5] however, mechanical detection methods have also been reported.[6,7]

We focus on the thermal detection method to extend the frequency range of angle-dependent ESR spectroscopy. Among a variety of electron spin resonance measurement techniques, thermal detection is a relatively old technique that was originally demonstrated in the year 1966.[8] It utilizes the fact that the energy absorbed by a sample during an ESR measurement is converted into heat during the spin-lattice relaxation process. In the first experiment by Schmidt and Solomon, ESR was detected as a change in the resistance of a thin copper wire to which the sample was attached.[8] After their experiments at room temperature, bolometric detection was extended to the lower temperature down to the dilution refrigerator temperature range using various temperature sensors.[9–11] It was shown that the sensitivity was greatly improved in the low temperature region, where the specific heat of the material is small. In addition to the measurements using a temperature sensor, there have been many methods that measure the change in temperature-dependent physical quantities. Examples of such more

indirect thermal detection use the temperature dependence of the sample resistance,[12,13] magnetization,[14,15] and the thermoacoustic effect.[16]

Since heating is a universal phenomenon for magnetic resonance, the thermal detection method can be applied to various types of samples. However, there have been few reports on thermal detection in recent years. This is probably due to the fact that its advantage has been diminished with the establishment of the resonator method around X-band, where most of the earlier experiments were performed. Nevertheless, thermal detection is still attractive in the frequency range above 100 GHz, where the use of cavity resonators is not easy and broadband methods are desired. In fact, we have previously developed a highly sensitive force detection system that detects the magnetization change caused by ESR heating[15] and demonstrated that it is powerful for the study of the small volume samples.

In this work, we present a simple experimental setup for the thermally detected ESR in the millimeter/submillimeter range with the capability of magnetic field angle rotation. With a simple method based on the direct temperature measurement, we have succeeded in combining the features of high sensitivity (10^{12} spins/G), broad frequency ranges, and the ability of continuous angular rotation, which are difficult to achieve with conventional methods. We demonstrate its usefulness by the measurement of a Shastry–Sutherland quantum magnet $SrCu_2(BO_3)_2$.

II. EXPERIMENTAL

The temperature rise due to ESR heating is easily detected once the sample is insulated from the thermal bath. However, the higher the insulation, the longer it takes for the sample to reach a steady state. This makes it difficult to combine a sample temperature measurement with ESR spectroscopy, which acquires spectra while sweeping a magnetic field at a typical sweep rate of 0.1–0.5 T/min. Therefore, we developed a cantilever-type device in which the sample and the heat bath are connected by a material with known thermal properties. Figure 1 shows the schematic of our device. The cantilever was cut from a 50 μm thick BeCu foil and was attached to a sapphire thermal bath using GE 7031 varnish. The typical cantilever dimensions are $l \times w \times t = 2 \times 0.5 \times 0.05$ mm^3. The sample was mounted at the end of the cantilever with GE7031 or Apiezon N grease. When the ESR conditions are met, the sample absorbs the energy of the electromagnetic wave and gets heated up during the spin-lattice relaxation process. Almost all the heat is released to the cantilever under a high vacuum of $< 10^{-4}$ Pa. As a result, ESR can be detected by measuring the temperature difference, ΔT, between the end of the cantilever and the heat bath. We used a thin $AuFe_{0.07}$-chromel differential thermocouple for ΔT measurement. The diameters of $AuFe_{0.07}$ and chromel wire are 21 and 25 μm, respectively. This combination is commonly used in low temperature environments because it maintains a thermopower of $S = 10$–$20\ \mu$V/K even below 20 K. The thermocouple junction on the high temperature side was soldered with indium to make a strong thermal contact near the cantilever end, while the low temperature side was fixed to the sapphire block using GE7031 or Stycast 1266 epoxy. The temperature and magnetic field dependence of S was calibrated prior to the ESR measurement.

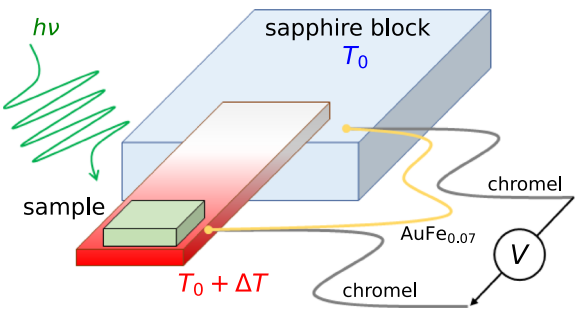

FIG. 1. Schematic of the cantilever-shaped device for thermal ESR detection.

The temperature difference in the steady state ΔT_∞ can be estimated from the Fourier law,[17]

$$\Delta T_\infty = \frac{P_{\mathrm{ESR}} l}{\kappa_{\mathrm{BeCu}} wt}, \tag{1}$$

where P_{ESR} and κ_{BeCu} are the absorbed power by ESR and the thermal conductivity of BeCu, respectively. Note that this relationship is valid only when the heat current is homogeneous between two thermocouple junctions. In our setup, the heat current is somewhat inhomogeneous because one of the junctions is fixed to the insulating thermal bath to maximize the signal and to avoid electric shorting of the junctions. Therefore, Eq. (1) provides only a rough estimation. Using $\kappa_{\mathrm{BeCu}} = 10$ W/mK at 20 K,[18] $\Delta T_\infty = 8$ mK is expected when $P_{\mathrm{ESR}} = 1\ \mu$W. This temperature difference corresponds to the thermovoltage of ~120 nV. We measured this small voltage using a nanovoltmeter (model 2182A, Keithley Instruments, Inc.) or a lock-in amplifier (Stanford Research Systems, Inc.) after amplifying it with two low-noise amplifiers (SA-200F3 and SA-410F3, NF Corporation) connected in series with a total gain of 10^4.

The measurements were performed in the 10 T split-pair superconducting magnet (SM4000-10, Oxford instruments) equipped with a variable temperature insert (VTI) whose inner diameter is 25 mm. Figure 2 shows the high vacuum probe designed for use in the VTI. The sample stage consisting of oxygen-free copper is thermally insulated from the brass flange, which is cooled to the VTI temperature using thin stainless tubes. The temperature of the sample stage is controlled independently of the VTI temperature using a 25Ω manganin wire heater and a Cernox® temperature sensor. The stability of the sample stage temperature is $|\delta T| < 1$ mK below 30 K, and $|\delta T|$ gradually increases as T increases. Prior to the measurement, the probe was sealed with vacuum grease and evacuated using a turbo-molecular pump to below 10^{-4} Pa. Thereafter, the sample stage was slowly cooled in the VTI for more than 4 h. The lowest VTI temperature is 1.4 K, whereas an ESR measurement is possible only above 1.8 K owing to Joule heating of the sample stage by electromagnetic waves.

An electromagnetic wave was introduced by a circular stainless-steel waveguide. This waveguide was gently curved to block the thermal radiation from the environment. As an electromagnetic wave source, we used an active multiplier chain (AMC) (WR6.0IAMC-, Virginia diodes, Inc.), whose output power is $P_{\mathrm{out}} > 50$ mW at the millimeter wave frequency of $f = 120$–190 GHz. In the higher frequency range, we combined the AMC with a frequency doubler

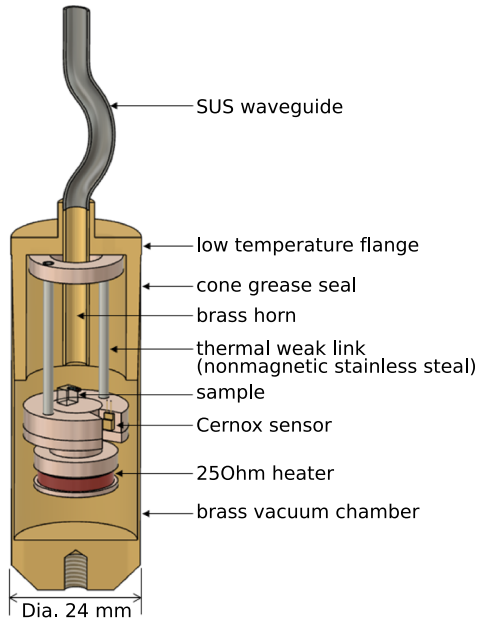

FIG. 2. Low temperature part of high vacuum probe for thermally detected ESR measurement. The wiring and electric terminals are not shown for clarity.

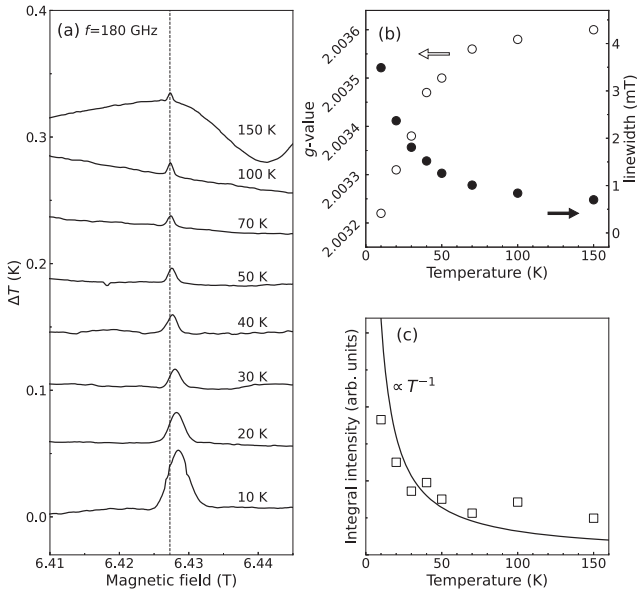

FIG. 3. (a) ESR spectra obtained as a function of ΔT for different magnetic fields for 10 μg of diphenylpicrylhydrazyl (DPPH) powder. The measurements were acquired between temperatures of 10 and 150 K at a millimeter wave frequency of 180 GHz. The dashed line shows the resonance field at 150 K. (b) Temperature dependence of the g-value (open squares) and linewidth (closed circles) obtained from the spectra in (a). (c) Temperature dependence of integral absorption intensity calculated assuming homogeneous heat current along the cantilever. The open squares show the experimental data. The solid line shows the Curie law.

when f = 260–330 GHz and with a tripler when f = 400–550 GHz (WR3.4×2 and WR1.9×3, Virginia diodes, Inc.). The typical conversion efficiency is 8% for WR3.4×2 and 3% for WR1.9×3. For measurements near the lowest temperature, a manual attenuator was used to adjust the electromagnetic power to stabilize the stage temperature.

III. RESULTS AND DISCUSSION

A. Thermal detection method

Figure 3 shows the ESR spectra of 10 μg powder of 2,2-diphenyl-1-picrylhydrazyl (DPPH) for T = 10–150 K at f = 180 GHz. The magnetic field was swept slowly at a rate of 0.01 T/min, while the electromagnetic waves were continuously irradiated. The steady state was maintained during the sweep, which was confirmed by the fact that the line shape did not depend on the sweep direction of the magnetic field. We obtained all the spectra under a constant millimeter wave power to compare the signal intensities.

The resonance field corresponds to the g-value of DPPH (g = 2.0036). The linewidth is δB = 0.7 mT at T = 150 K. However, it broadens as the temperature decreases, and δB = 3.5 mT at T = 10 K. We also observed that the resonance field shifted at low temperatures, which corresponds to the change in the g-value, $\Delta g \simeq -0.0004$. It is known that the ESR spectrum of DPPH powder shows various temperature dependences according to the amount of solvent that is contaminated in the crystallization process or the volume of the adsorbed gas.[19] Since the sample is placed in a high vacuum environment during the measurements, we should take the former into the account. Although the details of the synthesis have not been provided by the manufacturer, we confirmed a sharp decrease in magnetization from around 10 K from our SQUID measurements, which is a characteristic feature of solvent-free polycrystals.[20] The reduction in magnetization is due to the formation of the antiferromagnetically coupled spin dimer. Therefore, the shift in the g-value and broadening of ESR linewidth at low temperatures are attributed to the evolution of spin correlation. A similar behavior has also been observed in the X-band measurement.[21]

ΔT becomes larger with decreasing T. Considering the temperature dependence of κ_{BeCu}, we can evaluate P_{ESR} from Eq. (1). We found that the integration intensity $I = \int P_{ESR} dH \propto \kappa_{\mathrm{BeCu}}(T) \int \Delta T dH$ increases toward lower temperatures, as shown in Fig. 3(c). It must be noted once again that Eq. (1) is not strictly true in our setup. Therefore, the calculated I does not agree well with the Curie law ($\propto T^{-1}$). We believe that this error can be eliminated if both junctions of the thermocouple are placed near the center of the cantilever beam, as in the standard thermal conductivity measurement method. In that case, however, the ESR signal intensity will be considerably reduced.

In DC measurements, there was a fluctuation of the baseline due to the temperature instability of the measurement system including the room temperature regime. To eliminate the drift and to enhance the sensitivity, we modulated the amplitude of the millimeter waves and detected the periodic temperature changes ΔT_{AC} using a lock-in amplifier. Figure 4(a) shows ESR spectra measured at T = 10 K with different modulation frequencies f_m. The high signal-to-noise ratio η = 280 was obtained at f_m = 3 Hz. Meanwhile, ΔT_{AC} rapidly decreased as f_m increased. This indicates that the modulation period is shorter than the thermal response time of the

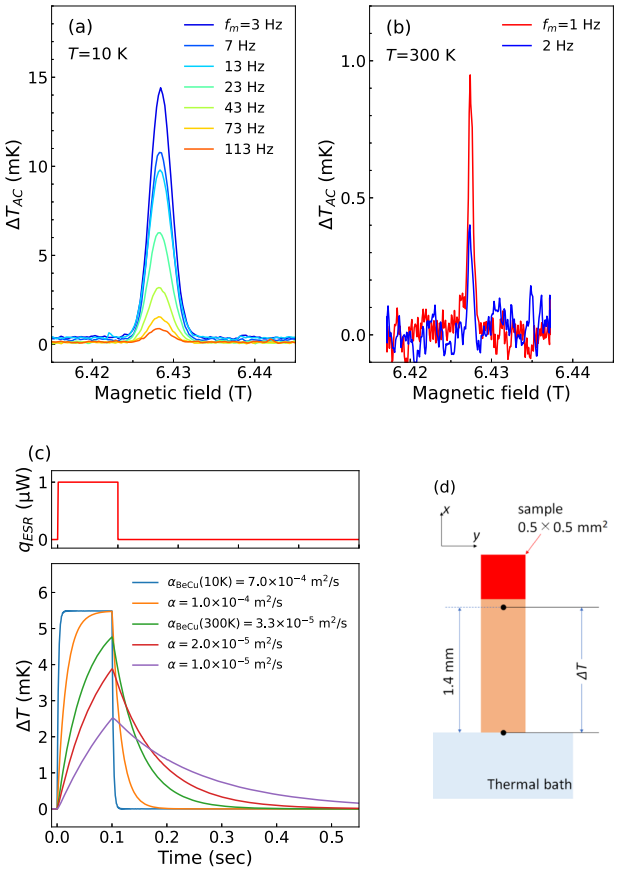

FIG. 4. (a) ESR spectrum of DPPH at T = 10 K and f = 180 GHz obtained with different f_m values. (b) Room temperature spectrum of DPPH. (c) Transient response of the temperature difference in the direction of the cantilever beam due to pulse heating of the sample assuming different thermal resistivities. The top panel shows the pulse waveform. The contact thermal resistance between the sample and the cantilever is neglected. (d) Dimensions of the cantilever used for the calculation in (c).

measurement system, i.e., the time from the start of ESR heating until the output of the thermocouple reaches a steady state. At high temperatures, the slower thermal response and weaker ESR absorption reduce η. Nevertheless, we observed the signal at T = 300 K at f_m = 1 Hz, as shown in Fig. 4(b).

The thermal response time of the cantilever itself, τ_c, can be estimated by calculating the transient response to the pulse heating by the following thermal equation:

$$\frac{\partial u(x,t)}{\partial t} = \alpha\left(\frac{\partial^2 u(x,t)}{\partial x^2} + \frac{\partial^2 u(y,t)}{\partial y^2}\right) + \frac{q_{\mathrm{ESR}}}{c\rho}, \tag{2}$$

where u is the temperature distribution inside the cantilever beam, q_{ESR} is the absorbed energy per unit area, and α, c, and ρ are the thermal diffusivity, specific heat, and density of the cantilever material, respectively. We assumed the sample and wire configuration depicted in Fig. 4(d) and used different α including the value for BeCu, $\alpha_{\mathrm{BeCu}}(10\ \mathrm{K}) = 7.0 \times 10^{-4}$ and $\alpha_{\mathrm{BeCu}}(300\ \mathrm{K}) = 3.3 \times 10^{-5}$ m^2/s. We found that ΔT exponentially decays with $\tau_c(10\ \mathrm{K}) = 2.2$ and $\tau_c(300\ \mathrm{K}) = 53$ ms after providing the heating pulse [Fig. 4(c)]. At both temperatures, τ_c^{-1} is larger than the modulation frequency at which the decay of ΔT_{AC} becomes significant. This indicates that factors other than the thermal properties of BeCu, such as the thermal contact between the sample and the cantilever and the thermal diffusion inside the thermocouple wire, are dominant in slowing down the thermal response.

The spin sensitivity, which represents the number of spins per 1 G of spectral width that can be detected with a signal-to-noise ratio of 1, is calculated to be $N_{\mathrm{spin}}/(\eta\delta B)$, where N_{spin} is the total spin number. We obtained a spin sensitivity of 1.8×10^{12} spins/G at 10 K and 1.3×10^{14} spins/G at 300 K. These sensitivity values are approximately two orders of magnitude higher than those obtained in the broadband transmission method and comparable to those of the force detection method.[15] The sensitivity can be enhanced by increasing the millimeter wave power as long as the rise in sample temperature is tolerated. We typically adjust the millimeter wave power so that $\Delta T/T < 0.01$. Under this condition, the upper limit of η inevitably becomes smaller at lower temperatures. However, the sensitivity is still sufficient for the measurement of the crystal, whose largest plane is smaller than 1×1 mm^2 as described in Sec. III B.

B. Application to angle-dependent HFESR spectroscopy

To demonstrate the application of thermal detection in the angular-dependent measurement, we measured ESR of a single crystal of $SrCu_2(BO_3)_2$ whose dimensions are $1 \times 0.8 \times 0.5$ mm^3. This tetragonal compound is composed of alternating Sr^{2+} and $CuBO_3^{2-}$ layers. In the $CuBO_3^{2-}$ layers, antiferromagnetically coupled Cu^{2+} ion dimers are orthogonally aligned via BO_3 [Fig. 5(a)]. The magnetic state is described by the Shastry–Sutherland model.[22,23] The ground state is the dimer singlet state at an ambient pressure, wherein the ratio of inter-dimer exchange interaction to intra-dimer exchange interaction is $J'/J \simeq 0.60$. The excited states have also been actively studied to explore the behavior near the quantum critical point, which appears near $J'/J \simeq = 0.66$.[24]

Figures 5(c) and 5(d) show the ESR spectra at 1.8 K at f = 470 and 540 GHz. The average power of the electromagnetic wave source and f_m were set to 0.3 mW and 3 Hz, respectively. The magnetic field was rotated in the (010)-plane, and θ was defined as the angle between the magnetic field and a-axis. The observed signal corresponds to the transition from the ground state to the one-dimer triplet state, which is the first excited state having a gap frequency of ~ 720 GHz [Fig. 5(b)]. We observed that the absorption, which was a single peak in $H//a$, splits as the magnetic field is rotated toward the c-axis.

For the analysis of the angle dependence, one should consider J, J', and the intradimer and interdimer Dzyaloshinskii–Moriya (DM) interaction $\boldsymbol{D}(\perp c)$ and $\boldsymbol{D}' = (0, 0, D'_{\perp})$. Among them, J' reduces the excitation energy of the triplet but does not contribute to the hopping up to the sixth order of J'/J.[25] The role of $\boldsymbol{D}$ is significant only at high fields, that is, near the critical field where the level mixing of the triplet and singlet states occurs. Taking these into account, the following Hamiltonian can be constructed by

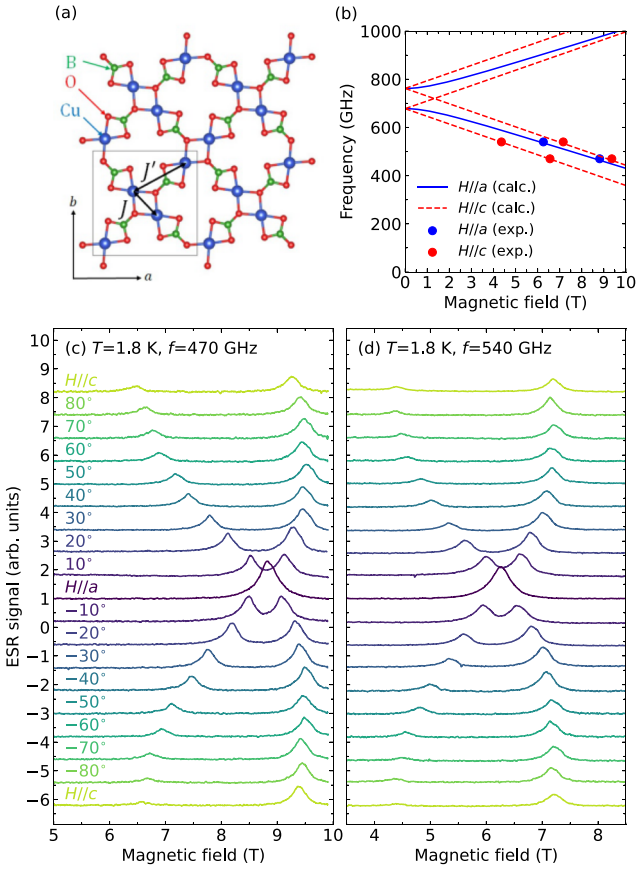

FIG. 5. (a) $Cu(BO)_3^{2-}$ layer of $SrCu_2(BO_3)_2$. J and J' are the intradimer and interdimer exchange interactions, respectively. (b) Relation between the resonance fields and the electromagnetic wave frequency (solid lines) for one-dimer triplet excitation. The closed dots correspond to the data shown in (c) and (d). [(c) and (d)] Field-angle dependent ESR spectra of $SrCu_2(BO_3)_2$ at T = 1.8 K at frequencies of 470 and 540 GHz. The magnetic field was swept at a rate of 0.5 T/min.

considering the triplet wave function as a basis based on the bond-wave formalism,[26,27]

$$H = \begin{pmatrix} A & C \\ C^{\dagger} & A \end{pmatrix}, \tag{3}$$

where

$$A = \begin{pmatrix} \tilde{J} & ig_z\mu_B H_z & 0 \\ -ig_z\mu_B H_z & \tilde{J} & ig_x\mu_B H_x \\ 0 & -ig_x\mu_B H_x & \tilde{J} \end{pmatrix} \tag{4}$$

and

$$C = \begin{pmatrix} 0 & 2D'_{\perp} & 0 \\ -2D'_{\perp} & 0 & 0 \\ 0 & 0 & 0 \end{pmatrix}. \tag{5}$$

The diagonal element $\tilde{J}$ in which J' is renormalized gives the triplet energy at zero field. We used the g-value (g_a = 2.05 and g_c = 2.28) determined in previous studies.[28,29] As shown in Fig. 6, both 470 and 540 GHz data are well fitted by the same parameters $\tilde{J}/h$ = 724 GHz and $D'_{\perp}/h$ = 21.9 GHz. These values are very close to those obtained by the inelastic neutron scattering experiment and are analyzed using the same analysis method.[27]

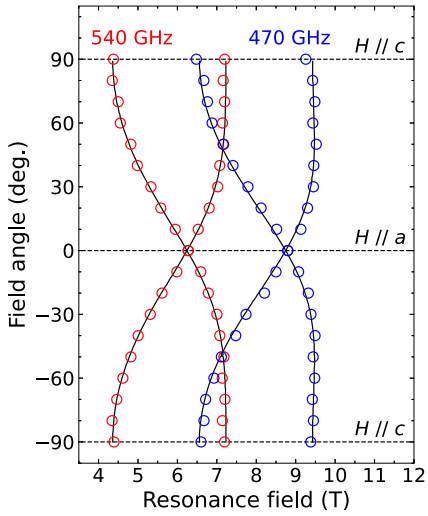

FIG. 6. Field-angle dependence of the resonance field of $SrCu_2(BO_3)_2$. The red and blue open circles are the experimental data at frequencies of 470 and 540 GHz. The solid lines are calculations with parameters $\tilde{J}/h$ = 724 GHz and $D'_{\perp}/h$ = 21.9 GHz.

In general, the transitions between energy levels with different spin quantum numbers are forbidden in the magnetic dipole transition mechanism. In this system, several possible mechanisms have been proposed, which make the transition probability finite, such as the effects of DM interaction[30] and the magnetoelectric coupling.[31] The transition probabilities due to these mechanisms are material-dependent, and in many cases, they are much smaller than the simple paramagnetic resonance. Therefore, our high-sensitivity method is a powerful tool for the study of various types of magnetic excitations (even those with small transition probabilities) in quantum spin systems.

IV. FUTURE DEVELOPMENT

Finally, we mention the prospects for further expansion of the measurement window. In the measurement of $SrCu_2(BO_3)_2$ at 540 GHz, the minimum detectable number of spins, calculated from the peak on the high field side, are of the order of 10^{13} spins per 0.1 mT spectral width. Considering the small transition probability, it is expected that a spin sensitivity of 10^{12} spins/G can be obtained for a paramagnetic sample. This indicates that the measurement can be performed at further higher frequencies, wherein the output intensity of the light source decreases. The extension of the magnetic field range is also expected to be straightforward. Since the cantilever device is small enough to be mounted on a gear-driven rotating mechanism in a solenoid-type magnet, it will be possible to extend the magnetic field range beyond 20 T.[32]

The sensitivity at room temperature is not very high. However, there is still scope for improvement by adopting the more appropriate thermocouple and cantilever materials. For example, the chromel-constantan thermocouple is effective because its thermopower is three times larger than that of the chromel-$AuFe_{0.07}$ thermocouple near room temperature.

We are also interested in the application to the measurement of conducting samples. In the microwave frequency range, the surface resistance measurement using a bolometric technique has been reported.[33] Since the surface resistance is proportional to $\sqrt{f}$, the energy loss at the surface increases at high frequencies. In this case, it may be necessary to separate the magnetic resonance signal from other resonance phenomena such as cyclotron resonance.

V. CONCLUSIONS

In this article, we have reported an ESR technique based on thermal detection. A cantilever-shaped device allowed us to measure the temperature change in the sample caused by ESR at a field sweep rate of ~0.5 T/min, which is standard for high frequency ESR experiments. The spin sensitivity was enhanced up to 1.8×10^{12} spins/G at $T = 10$ K by the modulation method. This value is comparable to the sensitivity of force detection and is sufficient for the measurements on submillimeter-sized samples. The most notable feature of this method is that it enables the acquisition of precise field-angle dependence at multiple frequencies up to above 500 GHz. We demonstrate its usefulness by observing the field-angle dependence of the excitation energy of the dimer triplet state in $SrCu_2(BO_3)_2$. It is expected that the frequency and magnetic field ranges will be further extended. Since there is no other method that combines the simplicity, high sensitivity, and angle-resolved measurement capability, we believe that our technique will make a significant contribution to the study using ESR spectroscopy.

ACKNOWLEDGMENTS

We would like to thank Professor Y. Koike (Tohoku University) and Professor K. Kudo (Osaka University) for the sample preparation of $SrCu_2(BO_3)_2$. This study was partly supported by the JSPS KAKENHI (Grant Nos. 19K03746 and 19K21852) and JST, PRESTO Grant No. JPMJPR18I6, Japan.

DATA AVAILABILITY

The data that support the findings of this study are available from the corresponding author upon reasonable request.

REFERENCES

[1] C. P. Poole, Jr., *Electron Spin Resonance*, 2nd ed. (Dover, New York, 1996).
[2] M. Motokawa, H. Ohta, and N. Maki, Int. J. Infrared Millimeter Waves **12**, 149 (1991).
[3] S. Takahashi and S. Hill, Rev. Sci. Instrum. **76**, 023114 (2005).
[4] M. Kimata, K. Koyama, H. Ohta, Y. Oshima, M. Motokawa, H. Nishikawa, K. Kikuchi, and I. Ikemoto, Jpn. J. Appl. Phys., Part 1 **44**, 4930 (2005).
[5] G. Annino, M. Cassettari, M. Fittipaldi, and M. Martinelli, J. Magn. Reson. **176**, 37 (2005).
[6] E. Ohmichi, S. Hirano, and H. Ohta, J. Magn. Reson. **227**, 9 (2013).
[7] H. Takahashi, K. Ishimura, T. Okamoto, E. Ohmichi, and H. Ohta, Rev. Sci. Instrum. **89**, 036108 (2018).
[8] J. Schmidt and I. Solomon, J. Appl. Phys. **37**, 3719 (1966).
[9] L. Janssens and J. Witters, J. Appl. Phys. **41**, 2064 (1970).
[10] W. S. Moore and T. M. Al-Sharbati, J. Phys. D: Appl. Phys. **6**, 367 (1973).
[11] M. Mertig, E. Tjukanov, S. A. Vasilyev, A. Ya. Katunin, and S. Jaakkola, J. Low Temp. Phys. **100**, 45 (1995).
[12] M. Guéron and I. Solomon, Phys. Rev. Lett. **15**, 667 (1965).
[13] Y. Toyoda and Y. Hayashi, J. Phys. Soc. Jpn. **33**, 718 (1972).
[14] J. Moreland, M. Löhndorf, P. Kabos, and R. D. McMichael, Rev. Sci. Instrum. **71**, 3099 (2000).
[15] H. Takahashi, T. Okamoto, K. Ishimura, S. Hara, E. Ohmichi, and H. Ohta, Rev. Sci. Instrum. **89**, 083905 (2018).
[16] R. L. Melcher, Appl. Phys. Lett. **37**, 895 (1980).
[17] J. H. Lienhard IV and J. H. Lienhard V, *A Heat Transfer Textbook* (Dover Publications, New York, 2019).
[18] E. D. Marquardt, J. P. Le, and R. Ray, "Cryogenic material properties database," in *Cryocoolers 11* (Springer, Boston, MA, 2001), p. 681.
[19] N. D. Yordanov, Appl. Magn. Reson. **10**, 339 (1996).
[20] D. Zili *et al.*, J. Magn. Res. **207**, 34 (2010).
[21] N. Matsumoto and N. Itoh, Anal. Sci. **34**, 965 (2018).
[22] H. Kageyama, K. Yoshimura, R. Stern, N. V. Mushnikov, K. Onizuka, M. Kato, K. Kosuge, C. P. Slichter, T. Goto, and Y. Ueda, Phys. Rev. Lett. **82**, 3168 (1999).
[23] B. S. Shastry and B. Sutherland, Physica B+C **108**, 1069 (1981).
[24] T. Sakurai, Y. Hirao, K. Hijii, S. Okubo, H. Ohta, Y. Uwatoko, K. Kudo, and Y. Koike, J. Phys. Soc. Jpn. **87**, 033701 (2018).
[25] S. Miyahara and K. Ueda, Phys. Rev. Lett. **82**, 3701 (1999).
[26] J. Romhányi, K. Totsuka, and K. Penc, Phys. Rev. B **83**, 024413 (2011).
[27] P. A. McClarty, F. Krüger, T. Guidi, S. F. Parker, K. Refson, A. W. Parker, D. Prabhakaran, and R. Coldea, Nat. Phys. **13**, 736 (2017).
[28] H. Nojiri, H. Kageyama, K. Onizuka, Y. Ueda, and M. Motokawa, J. Phys. Soc. Jpn. **68**, 2906 (1999).
[29] H. Nojiri, H. Kageyama, Y. Ueda, and M. Motokawa, J. Phys. Soc. Jpn. **72**, 3243 (2003).
[30] T. Sakai, J. Phys. Soc. Jpn., Suppl., B **72**, 53 (2003).
[31] S. Kimura, M. Matsumoto, M. Akaki, M. Hagiwara, K. Kindo, and H. Tanaka, Phys. Rev. B **97**, 140406(R) (2018).
[32] T. Sakurai, S. Kimura, M. Kimata, H. Nojiri, S. Awaji, S. Okubo, H. Ohta, Y. Uwatoko, K. Kudo, and Y. Koike, J. Magn. Reson. **296**, 1 (2018).
[33] P. J. Turner, D. M. Broun, S. Kamal, M. E. Hayden, J. S. Bobowski, R. Harris, D. C. Morgan, J. S. Preston, D. A. Bonn, and W. N. Hardy, Rev. Sci. Instrum. **75**, 124 (2003).